Title

The Antiviral RNA Interference Response Provides Resistance to Lethal Arbovirus Infection and Vertical Transmission in Caenorhabditis elegans

Journal

Current Biology, 27(6)

ISSN

0960-9822

Authors

Gammon, Don B

Ishidate, Takao

Li, Lichao

et al.

Publication Date

2017-03-01

DOI

10.1016/j.cub.2017.02.004

HHS Public Access

Author manuscript

Curr Biol. Author manuscript; available in PMC 2018 March 20.

Published in final edited form as:

Curr Biol. 2017 March 20; 27(6): 795–806. doi:10.1016/j.cub.2017.02.004.

The Antiviral RNA Interference Response Provides Resistance to Lethal Arbovirus Infection and Vertical Transmission in *Caenorhabditis elegans*

Don B. Gammon[1], **Takao Ishidate**[1], **Lichao Li**[2], **Weifeng Gu**[2], **Neal Silverman**[3], and **Craig C. Mello**[1,4,*]

[1]University of Massachusetts Medical School, RNA Therapeutics Institute, Worcester, MA, 01605, USA

[2]University of California, Riverside, Department of Cell Biology and Neuroscience, Riverside, CA, 92521, USA

[3]University of Massachusetts Medical School, Department of Medicine, Worcester, MA, 01605, USA

[4]Howard Hughes Medical Institute, University of Massachusetts Medical School, Worcester, MA, 01605, USA

SUMMARY

The recent discovery of the positive-sense ssRNA Orsay virus (OV) as a natural pathogen of the nematode, *Caenorhabditis elegans*, has stimulated interest in exploring virus-nematode interactions. However, OV infection is restricted to a small number of intestinal cells, even in nematodes defective in their antiviral RNA interference (RNAi) response, and is neither lethal nor vertically transmitted. Using a fluorescent reporter strain of the negative-sense ssRNA vesicular stomatitis virus (VSV), we show that microinjection of VSV particles leads to a dose-dependent, muscle tissue-tropic, lethal infection in *C. elegans*. Furthermore, we find nematodes deficient for components of the antiviral RNAi pathway, such as Dicer-related helicase 1 (DRH-1), to display hypersusceptibility to VSV infection as evidenced by elevated infection rates, virus replication in multiple tissue types, and earlier mortality. Strikingly, infection of oocytes and embryos could also be observed in *drh-1* mutants. Our results suggest that the antiviral RNAi response not only inhibits vertical VSV transmission but also promotes transgenerational inheritance of antiviral

*Corresponding author and Lead Contact: Please address all correspondence to craig.mello@umassmed.edu. Tel. (508) 856-3692; Fax (508) 856-2950.

SUPPLEMENTAL INFORMATION

Supplemental Information includes six figures (S1–S6) and Supplemental Experimental Procedures.

AUTHOR CONTRIBUTIONS

Conception and design: DBG, TI, WG, NS, CCM. Acquisition of data: DBG, TI, LL. Analysis and interpretation of data, DBG, TI, LL, WG, NS, CCM. Drafting or revising the article: DBG, TI, LL, WG, NS, CCM.

immunity. Our study introduces a new, *in vivo* virus-host model system for exploring arbovirus pathogenesis and provides the first evidence for vertical pathogen transmission in *C. elegans*.

Keywords

Caenorhabditis elegans; vesicular stomatitis virus; RNA interference; small RNAs; virus-host interactions; vertical transmission; transgenerational inheritance; antiviral immunity

INTRODUCTION

The genetic tractability, ease of culture, and susceptibility to a variety of bacterial and fungal pathogens [1, 2], has made *C. elegans* attractive for exploring microbe-host interactions. However, due to a lack of convenient experimental systems, relatively few studies have explored virus-*C. elegans* interactions. Initial studies investigating virus-*C. elegans* interactions used primary cell cultures and defined an antiviral role for the nematode RNA interference (RNAi) response [3, 4].

RNAi is a highly conserved mechanism of gene silencing that contributes to antiviral defense in insects [5], plants [6], and mammals [7, 8]. In *C. elegans*, the antiviral RNAi response is initiated after recognition and cleavage of viral double-stranded RNAs by a complex consisting of Dicer-related helicase 1 (DRH-1), DCR-1, and RDE-4, into 23 nucleotide (nt)-long primary small interfering RNAs (siRNAs) [9]. These duplex siRNAs are then loaded into the primary Argonaute protein RDE-1 and one strand of the duplex is lost. These RDE-1-primary siRNA complexes then recruit RNA-dependent RNA polymerase complexes to viral RNA targets where they generate secondary siRNAs termed “22Gs”, which are typically 22 nts long and contain 5′ guanines [10, 11]. These 22Gs then complex with, and guide, secondary Argonautes to complementary viral single-stranded (ss) RNA targets (e.g. mRNAs or genomes) resulting in Argonaute-mediated target cleavage and inhibition of virus replication [9].

Despite initial insights into virus-*C. elegans* interactions provided by primary cell culture studies, these cultures have limited utility because they are technically-challenging to generate and may not be representative of infection in animals. To investigate virus-*C. elegans* interactions *in vivo*, a nematode strain encoding a Flock House virus replicon was created by Lu et al [12]. Although this replicon system has identified host factors, such as DRH-1 [13], that restrict virus replication, it cannot identify nematode factors influencing aspects of the viral life cycle that would only be afforded with a bona fide viral pathogen (e.g. transmission, entry, exit, etc.) [14].

More recently, the positive-sense ssRNA Orsay virus (OV) was described as a natural pathogen of *C. elegans* [14]. The discovery of OV represents an important step in defining virus-nematode interactions, however, this model also possesses limitations. First, OV infection is limited to 1–6 intestinal cells, even during infection of RNAi-deficient animals [15]. Therefore, identifying antiviral factors specific to non-intestinal tissues with the OV model may be difficult. Second, because OV infection is not lethal [14], scoring the minor pathological features of infection can be challenging. Third, recombinant OV strains

expressing fluorescent or quantifiable reporter genes are unavailable, making analysis of OV replication limited to PCR or immunofluorescence-based methods. Finally, because OV is not vertically transmitted [14], this model may be unsuitable for identifying immunity mechanisms guarding against vertical transmission.

Given the shortcomings of current virus-*C. elegans* model systems, we asked whether an alternative system could be established using the negative-sense ssRNA vesicular stomatitis virus (VSV). VSV is a member of the arboviruses, a group of emerging viral pathogens that are transmitted by arthropods to vertebrate hosts. The wide availability of reverse genetic and immunological tools for VSV [16, 17] makes it convenient for studying arboviral disease mechanisms relevant to human and animal health [18, 19]. Furthermore, because VSV can replicate in *C. elegans* primary cells [3, 4], we thought it possible that VSV could infect *C. elegans* animals.

Here we show that microinjection of VSV particles produces a lethal infection in *C. elegans*. We further show that the susceptibilities of animals to infection, the tissues infected, and animal survival, are dependent upon virus dose, culturing conditions, and host genetic background. We also establish a role for the nematode antiviral RNAi pathway in restricting arbovirus replication and pathogenesis. Finally, we use this model to provide the first evidence for vertical transmission in *C. elegans* and implicate the antiviral RNAi response in both inhibiting vertical transmission and promoting transgenerational inheritance of antiviral immunity.

RESULTS

Microinjection of VSV into *C. elegans* results in an infection primarily restricted to muscle tissue

To determine if VSV could infect *C. elegans*, we microinjected wild-type (N2 strain) adults with a recombinant VSV strain encoding the fluorescent reporter dsRED (VSV-dsRED) [20]. We targeted the body cavity and intestinal tissue just posterior to the terminal bulb of the pharynx for injections. After microinjection, we observed a prominent dsRED signal in animals that was both above background signals in mock-infected animals and significantly different from autofluorescence observed in intestinal tissues (Figure 1A). Microinjection of VSV-dsRED into transgenic animals expressing GFP under a neuronal promoter [21] revealed only a minor overlap of GFP and dsRED signals in head neurons (Figure 1B–C). However, significant overlap in dsRED and GFP signals was observed throughout infected transgenic animals expressing GFP under a muscle-specific promoter ([21]; Figure 1D), with clear infection of body wall muscle in the head and tail (Figure 1E). We could also establish VSV-dsRED infections in the Hawaiian isolate (CB4856) of *C. elegans* (Figure S1A) and in *Caenorhabditis briggsae* (Figure S1B). Interestingly, whereas both the N2 and Hawaiian animals displayed infection rates of 85–90%, only ~20% of *C. briggsae* animals displayed dsRED signal by 72 hours post-infection (hpi), suggesting that *C. briggsae* may be more resistant to infection (Figure S1C).

Loss of DRH-1 function results in hypersusceptibility to lethal VSV infection

Previous Flock house virus replicon [13] and OV [9] studies have implicated DRH-1 in the restriction of positive-sense ssRNA virus replication in *C. elegans*. DRH-1 functions in a similar manner as homologous mammalian RIG-I-like helicases (RLHs) which sense cytosolic viral RNA signatures and subsequently trigger antiviral response programs [9, 22]. While mammalian RLHs and DRH-1 both trigger an antiviral response upon viral RNA recognition, mammalian RLHs trigger the interferon response [23], whereas DRH-1 promotes the initiation of the *C. elegans* antiviral RNAi response [9, 13].

To determine if DRH-1 is involved in sensing negative-sense ssRNA virus infection, we challenged animals carrying a loss-of-function mutation in *drh-1* with VSV-dsRED and compared the dsRED pattern to N2 infections. Interestingly, *drh-1* worms displayed infection in multiple tissues not involved in N2 infections such as intestinal tissue (Figure 2A). To further compare dsRED signals in N2 and *drh-1* strains, we microinjected either a low [10^2 plaque-forming units (PFU)] or high (10^4 PFU) dose of VSV-dsRED into either strain and then measured signals in either whole animals (Figure 2B) or specific tissues (Figure 2C–F) 48 hpi. Whole body dsRED measurements indicated that *drh-1* animals displayed ~5- and 18-fold higher signals than mock-infected animals at the 10^2 and 10^4 PFU doses, respectively. In contrast, dsRED signals in N2 animals were either essentially identical to or ~three-fold higher than mock-infected animals at these respective doses (Figure 2B). Measurement of dsRED signals in individual tissues revealed a similar pattern with *drh-1* animals presenting with ~4–10-fold higher signals at the 10^2 PFU dose and ~17–51-fold higher signals at the 10^4 PFU dose compared to mock-infected animals. Significant N2 dsRED signals were typically only observed with 10^4 PFU treatments and were ~3–7-fold higher than mock-infected animals. Animals were scored as infected if their whole body dsRED signals were at least two-fold higher than mock-infected animals by 48 hpi. Using this cutoff, we found that at a dose of 10^4 PFU, 100% of both N2 and *drh-1* animals scored as infected. In contrast, no N2 and 80% of *drh-1*, animals scored as infected in 10^2 PFU treatments (Figure 2G). However, when only vulval tissue dsRED signals were used to score infection in 10^2 PFU treatments, ~30% of N2 animals scored as infected (Figure S2), suggesting that this tissue may be a more reliable indicator of low-level infections. These results suggest that higher viral doses allow for viral replication to reach a threshold at which dsRED signals become detectable by 48 hpi in both N2 and *drh-1* strains. However, at lower viral doses, N2 animals may be more capable of suppressing VSV-dsRED replication and hence are not scored as infected by 48 hpi. Importantly, we confirmed that the elevated dsRED signal observed in *drh-1* animals reflected bona fide VSV transcription using RT-PCR (Figure S3; [24]).

To examine viral susceptibilities of N2 and *drh-1* strains further, we tracked animals that had been microinjected with 10^2, 10^3, or 10^4 PFU of VSV-dsRED for infection rate (Figure 2H) and survival (Figure 2I). The maximal number of infected animals in each injected group was reached by 48 hpi with the exception of N2 animals injected with 10^2 PFU, which took until 96 hpi (Figure 2H). The 10^2, 10^3, and 10^4 PFU doses resulted in infection of 25%, 50%, and 85% of N2 animals, respectively. In contrast, these doses resulted in 80%, 95%, and 100% infection rates in *drh-1* animals (Figure 2H). Given that infection rates in several

treatments never achieved 100%, it is likely that horizontal transmission of VSV between adults is inefficient.

We used lifespan assays (Figure 2I) to estimate the time at which 50% of animals in each treatment had died [expressed as lethal time 50 (LT_{50}) in hpi]. We also calculated 95% confidence intervals (CIs) for each LT_{50} and in cases where 95% CIs of two different LT_{50} values did not overlap, these two values were deemed statistically different ($P<0.05$). The LT_{50} (95% CI) for mock-infected N2 animals [250 hpi (236-265 hpi)] was not significantly different from mock-infected *drh-1* mutants [240 hpi (228-252 hpi)]. However, both N2 and *drh-1* animals had significantly lower LT_{50} values when infected with VSV-dsRED at any of the three doses used, suggesting that VSV infection is ultimately lethal. However, N2 animals survived for significantly longer periods of time than *drh-1* animals injected with the same viral dose. For example, at a dose of 10^2 PFU, the LT_{50} (95% CI) for N2 animals was 220 hpi (210-228 hpi) versus 112 hpi (104-119 hpi) for *drh-1* animals. This trend was also observed at the 10^3 PFU dose, with LT_{50} (95% CI) for N2 animals being 176 hpi (166-186 hpi) versus 121 hpi (116-127 hpi) for *drh-1* animals and at the 10^4 PFU dose [N2 = 168 hpi (162-174 hpi) versus *drh-1* = 106 hpi (99-112 hpi)]. These results suggest that *drh-1* animals suffer higher infection rates and reduced survival times compared to N2 animals.

A small RNA response is generated upon VSV infection

We next used deep-sequencing to determine if small RNAs (17–30 nts in length) were generated in response to VSV-dsRED infection. Small RNAs that mapped to the VSV-dsRED genome are shown in Figure 3A. These RNAs were virtually absent from uninfected animals (data not shown). In N2 libraries, small RNAs corresponding to the antisense (or genomic) strand of VSV-dsRED were ~29-fold more abundant than those mapping to the sense (antigenomic) strand (Figure 3B–C). Both antisense and sense RNAs were characterized by a peak length of 22 nts and a strong preference for G at their 5′ ends, and thus likely represent 22Gs. Consistent with a defect in the initiation of an antiviral RNAi response, ~four-fold fewer viral small RNAs were detected in *drh-1* animals than in N2 infections. Furthermore, while both antisense and sense small RNAs from *drh-1* animals also displayed a bias for 5′G residues, a clear 22 nt peak length was only observed among antisense small RNAs (Figure 3D–E). In addition, *drh-1* antisense small RNAs were only two-fold more abundant than sense RNAs. These results suggest that both N2 and *drh-1* animals raise a small RNA response to VSV-dsRED infection but that *drh-1* animals may be impaired in generating antisense small RNAs.

Development of a luciferase assay for VSV replication in *C. elegans*

To further characterize VSV infection dynamics, we created a simple, quantitative assay to assess VSV replication. To do this, we employed a recombinant VSV strain encoding a firefly luciferase (LUC) gene under a viral promoter (VSV-LUC; [25]) along with chemiluminescent LUC assays to measure VSV gene expression. LUC activity detected from VSV-LUC infections closely mirrors virion production and serves as a convenient and sensitive assay for virus production [24]. To test the utility of these assays, we microinjected groups of N2 or *drh-1* animals with VSV-LUC and collected equal numbers of animals at various times post-infection. Although light unit (LU) signals from infected N2 animals

were ~600-fold higher than from mock-infected animals by 24 hpi, these signals only increased by ~two-fold by 72 hpi (Figure 4A). In contrast, LU signals from VSV-LUC-infected *drh-1* animals were ~8800-fold higher than from mock-infected animals by 24 hpi and these signals increased by ~7-fold by 72 hpi. Trends observed in LUC assays were further confirmed by immunoblotting (Figure 4B). While we were unable to detect LUC protein from infected N2 lysates, we did detect a small amount of VSV Matrix structural protein (Figure 4B). In contrast, abundant LUC and Matrix proteins were detected in VSV-LUC-infected *drh-1* lysates (Figure 4B). Collectively, these data show that LUC assays provide a sensitive and convenient method to assess VSV replication in *C. elegans*.

VSV replication and infection and mortality rates are temperature-dependent

To determine if temperature influences VSV replication, we measured LU signals from VSV-LUC-infected animals cultured at 15, 20, or 25°C. LU signals were significantly higher when either N2 or *drh-1* animals were cultured at 25°C as compared to 15°C ($P<0.05$). Although not statistically different, LU signals from 20°C incubations trended towards being higher than signals from 15°C incubations (Figure 4C).

To investigate if temperature affected infection or mortality rates, we challenged animals with VSV-dsRED and then monitored animals for infection (Figure 4D) and survival (Figure 4E). Interestingly, incubation temperatures appeared to affect both the maximum percentage of animals infected and the timing of when these values were reached. For example, use of 15, 20, and 25°C incubation temperatures resulted in maximal infection rates of 38, 72, and 84% of N2 animals by 120, 72, and 48 hpi, respectively (Figure 4D). A similar trend was observed for *drh-1* animals (albeit with higher infection rates) such that 91, 95, and 100% of animals incubated at 15, 20, and 25°C scored as infected by 96, 48, and 24 hpi, respectively (Figure 4D).

Examination of survival rates suggested that LT_{50} values decrease with increasing temperature (Figure 4E). For example, LT_{50} (95% CI) values for infected N2 animals cultured at 15°C [408 hpi (403-413 hpi)], 20°C [384 hpi (380-388 hpi)], and 25°C [124 hpi (116-131 hpi)] were all significantly different from one another. The LT_{50} (95% CI) values for infected *drh-1* animals cultured at 15°C [257 hpi (239-274 hpi)], 20°C [191 hpi (177-205 hpi)], and 25°C [94 hpi (86-101 hpi)] also decreased with increasing temperature. Collectively, these results suggest that VSV replication and infection rates increase with increasing temperature while animal survival rates decrease.

Downstream components of the antiviral RNAi pathway are also required to restrict VSV infection

We next wanted to examine if strains with loss of function mutations in other RNAi pathway components display VSV hypersusceptibility. Using our LUC-based assays for viral replication, we found that, in addition to *drh-1* animals, the RNAi-defective strains, *rde-1* [26] and *rde-4* [26], also displayed significantly higher ($P<0.05$) VSV-LUC replication than N2 animals (Figure 4F), suggesting that these downstream components are also required to restrict viral replication. Although LU signals in RNAi-defective *C04F12.1* mutants [27] were ~8-fold higher than N2 animals, these values did not reach statistical significance

(P=0.1). Furthermore, strains deficient for SID-1 (required for systemic spreading of exogenous RNAi signals [28]), ALG-1 and ALG-2 (Argonautes involved in the microRNA pathway [29]), and PRG-1 (an Argonaute required for the Piwi-interacting RNA pathway [30]) did not display altered VSV-LUC susceptibilities (P>0.05).

We next asked if the enhanced viral replication observed in *rde-1* animals correlated with increased infection rates and reduced survival rates. While only 85% of N2 animals scored positive for infection, all *drh-1* and *rde-1* animals displayed dsRED signal by 48 hpi (Figure 4G). Furthermore, the LT_{50} (95% CI) values for both *drh-1* [119 hpi (105-133 hpi)] and *rde-1* [105 hpi (90-121 hpi)] animals were significantly lower than that of N2 animals [168 hpi (164-172 hpi)] but did not significantly differ from one another (Figure 4H). These data suggest that RNAi pathway components downstream of DRH-1 are also required for combating VSV infection.

DRH-1 is required for full immunity to vertical virus transmission

During our lifespan assays, we noticed that when we used NGM plates containing the DNA synthesis inhibitor, Fluorodeoxyuridine (FUdR), dsRED-positive embryos could often be observed with a fluorescence stereo zoom microscope on plates containing VSV-dsRED-infected *drh-1* animals (Figure 5A). FUdR has been shown to induce sterility and prevent egg hatching [31] and thus is useful when tracking adult nematodes over extended incubation periods. Importantly, FUdR does not impede VSV replication [32] and thus is not expected to directly affect viral replication. We further confirmed dsRED signals in embryos using differential interference contrast and fluorescence microscopy (Figure 5B). Furthermore, dsRED signals could be observed in oocytes (Figure S4A) and embryos (Figure S4B) within infected *drh-1* animals, suggesting that VSV-dsRED was entering and infecting germline tissues. We further confirmed VSV transcription in dsRED-positive embryos using RT-PCR (Figure S5).

Given our inability to detect dsRED-positive embryos in our initial experiments using normal NGM plates, we asked whether FUdR treatment might influence vertical transmission of VSV-dsRED. When cultured on control plates, both mock- and VSV-dsRED-infected N2 and *drh-1* animals produced a similar number of total progeny, suggesting that there were no virus- or strain-dependent differences. Similar results were obtained when injected animals were cultured on FUdR plates, albeit the total progeny sizes were reduced compared to control plates and a greater proportion of progeny were embryos (Figure 5C). Despite these reduced brood sizes, dsRED-positive embryos were only detected on FUdR plates containing *drh-1* animals (Figure 5D). Because only ~9% of embryos laid by infected *drh-1* animals displayed dsRED signal, we wanted to confirm that this was not simply a “jackpot” event that only occurred on *drh-1* plates by chance. Therefore, we repeated these experiments using larger numbers of N2 and *drh-1* adults and plated all VSV-dsRED-infected animals onto FUdR plates. Despite similar brood sizes between N2 and *drh-1* strains (Figure 5E), dsRED-positive embryos were again only detected on *drh-1* plates (Figure 5F).

We next asked if direct germline injection of VSV-dsRED might alter either overall or germline tissue-specific infection rates in N2 or *drh-1* animals after culturing animals on

FUdR. Interestingly, both strains displayed similar overall infection rates when either challenged by somatic or germline VSV-dsRED injections. In contrast, higher germline infection rates were observed when VSV-dsRED was directly injected into the germline (as oppose to the soma) for both N2 (0 versus 6%) and *drh-1* (24 versus 74%) animals (Figure S6A). These data suggest that direct injection of VSV-dsRED particles into the germline may overwhelm germline antiviral defenses that might otherwise be protective when VSV-dsRED must first spread from somatic tissues.

We next asked whether FUdR was still required to observe germline VSV-dsRED infection after direct challenge of the germline of *drh-1* animals. Strikingly, we observed similar germline infection rates in animals cultured on either control or FUdR-containing medium (Figure S6B). These data suggest that FUdR does not influence germline infection rates when VSV-dsRED is directly injected into the germline.

Collectively, these results show that VSV can be vertically transmitted to offspring, and that germline immunity to VSV infection can be influenced by the site of injection, the presence of FUdR in culturing medium, and DRH-1 function.

Inheritance of antiviral immunity after VSV infection

Although there is clear evidence for the transgenerational inheritance of RNAi responses generated by expression of foreign transgenes or the Flock House virus replicon in *C. elegans* [33, 34], inheritance of antiviral RNAi responses to OV remain controversial. Therefore, we were interested to determine if transgenerational immunity could be observed with our VSV model. To address this, we collected embryos from N2 animals that had either been mock- or VSV-dsRED-infected, allowed the resultant progeny to develop to adulthood, and then challenged these progeny with VSV-dsRED. As shown in Figure 6A, animals whose mother was previously exposed to VSV-dsRED exhibited a significantly lower infection rate than animals whose mother had been mock-infected ($P<0.01$). We then asked whether this inherited protection against infection could also be observed in *drh-1* animals. Interestingly, we found that both N2 and *drh-1* progeny animals displayed significantly reduced infection rates when they derived from infected mothers as opposed to mock-infected mothers ($P<0.05$) (Figure 6B).

In *C. elegans*, heritable antiviral immunity is thought to be mediated by small RNAs [34, 35], and our deep-sequencing results revealed a reduced, but not absent, small RNA response against VSV-dsRED in *drh-1* animals. Therefore, we thought it possible that the residual small RNA response (consisting primarily of 22Gs) in *drh-1* animals might be still capable of mediating a protective effect in resulting progeny. To address this, we made use of animals with an inactivating mutation in the *rde-3* gene, which encodes a putative nucleotidyl transferase required for 22G biogenesis [36, 37]. When challenged with 10^4 PFU of VSV-dsRED, *rde-3* animals displayed hypersusceptibility to infection as evidenced by infection of multiple tissues (Figure 6C), elevated infection rates (Figure 6D), and significantly reduced LT_{50} (91 versus 123 hpi) values compared to N2 animals (Figure 6E). Higher infection rates of *rde-3* animals were not only observed with higher doses (10^4 PFU) but also at lower (10^2 PFU) doses, further confirming the hypersusceptibility of *rde-3* animals to infection (Figure 6F). We then performed transgenerational immunity assays with

N2 and *rde-3* animals in which progeny from mock- or VSV-dsRED-infected mothers were challenged with either 10^2 or 10^4 PFU of VSV-dsRED and then scored for infection 72 h later. While N2 progeny derived from infected mothers displayed significantly reduced infection rates compared to those from mock-infected mothers when challenged with either low or high viral doses ($P<0.05$), this protective effect was lost in *rde-3* animals ($P>0.05$) (Figure 6G). Collectively, our results suggest that VSV infection of adult animals can lead to a heritable antiviral response that is dependent upon RDE-3 function.

DISCUSSION

An advantage of using VSV-dsRED microinjection for viral studies in *C. elegans* is that it allows the direct delivery of a known quantity of virus into an animal and the ability to score for infection and tissue involvement in real-time. The infection of RNAi-deficient mutants has revealed the ability of VSV to not only replicate in muscle tissue (as in N2 infections) but also in various tissues throughout the animal. The muscle-tropic nature of N2 infections was surprising given that in mouse models, VSV is typically neurotropic, although other tissues, including muscle, can become involved [19]. VSV neurotropism in mice might reflect tissue-specific differences in antiviral responses [19], and so it is possible that in *C. elegans*, muscle tissue antiviral responses may be less robust than in other tissues.

While previous studies have reported enhanced nodavirus replication in animals defective for RNAi pathway components such as DRH-1 [9, 13], RDE-1 [14], RDE-4 [14], it was unclear whether these factors contributed to the restriction of negative-sense ssRNA virus infection *in vivo*. A mammalian homolog of DRH-1, RIG-I, is required to initiate an interferon response to VSV infection in vertebrates [38]. The enhanced susceptibility of *drh-1* animals to VSV suggests that DRH-1 may act in an analogous manner, but instead initiate an antiviral response through the RNAi pathway. Our examination of small RNA responses in VSV-infected nematodes revealed a clear reduction in antisense 22Gs targeting VSV in *drh-1* mutants compared to N2 animals. A reduction in antisense 22Gs has also been described during OV infection of *drh-1* animals, suggesting that small RNAs targeting viral transcripts contribute significantly to the restriction of virus replication [9]. Interestingly, in both N2 and *drh-1* animals there were clear “hotspots” of small RNAs mapping to the 5′ end of the VSV genome. This has also been observed during small RNA responses against VSV in *Drosophila*, and has been attributed to the presence of self-complementary snapback defective interfering particles derived from 5′ end of the genome [39]. Curiously, although *Drosophila* Dicer proteins cleave these VSV snapback particles, the resulting siRNAs are, for unknown reasons, not loaded into Argonautes [39]. It has been postulated that these interfering particles may serve as a RNA decoy, allowing VSV evasion of RNAi machinery [39, 40]. It will be interesting to determine if VSV produces defective interfering particles in *C. elegans* and whether small RNAs targeting these particles are loaded into RDE-1.

Although SID-1 is required for the systemic spread of exogenous RNAi signals [28], *sid-1* mutants were as susceptible to VSV as N2 animals. This is consistent with previous virus studies in *C. elegans* [3, 33]. Whether another, unidentified, RNA transporter is required for mounting systemic RNAi responses to infection is unknown.

Interestingly, we found that VSV could infect the germline of *drh-1* animals and be vertically transmitted when somatically-injected animals were placed on FUdR-containing plates. How this DNA synthesis inhibitor might compromise germline immunity to infection is unknown. However, FUdR treatment can modulate resistance to thermal, hypertonic, and proteotoxic stresses, likely through alteration of gene expression [40]. Therefore, FUdR-induced inhibition of germline gene expression programs and/or stress responses that normally serve antiviral roles may promote germline infection and vertical transmission. However, because VSV could efficiently establish germline infection after direct injection into the germline in the absence of FUdR, these drug-induced effects may only be required to sensitize the germline to infection as the virus spreads from the soma. Direct injection of VSV into the germline may simply overwhelm germline antiviral responses, even without modulation by FUdR treatment. Importantly, no evidence was found for vertical transmission of other intracellular *C. elegans* pathogens such as microsporida [41] and OV [14]. Therefore, our model provides new opportunities to study vertical transmission in *C. elegans*.

Previous reports have demonstrated that administration of a mild stress (e.g. temporary starvation) to *C. elegans* can lead to enhanced protection of offspring from these same stressors, a phenomenon termed “transgenerational hormesis” [42, 43]. In some cases, this phenomenon can be mediated by small RNAs [43]. A previous report found transgenerational silencing of a Flock House virus transgene [34] and Sterken et al. [35] reported that OV-infected N2, but not RNAi-deficient, animals could transmit a heritable, protective antiviral response to their progeny. In contrast, Ashe et al. [33] did not find evidence for transgenerational immunity after OV infection. We found that prior exposure of N2 or *drh-1* animals to VSV led to significant reductions in the infection rates of their progeny when challenged with VSV. We were initially surprised by the inheritance of an antiviral response in *drh-1* animals, which is in contradiction with Sterken et al. [35]. However, because antiviral small RNA production in *drh-1* animals was reduced, but not eliminated, it is possible that these residual small RNAs may still confer protection to offspring. We attempted to detect small RNAs targeting VSV in the progeny from naïve or VSV-exposed mothers but were unable to observe significant quantities of viral small RNAs in these deep-sequencing experiments. It is unclear if viral small RNAs exist in progeny animals at too low a level for detection by our methods or whether the heritable antiviral effect is not mediated by small RNAs. We favor the former scenario as *rde-3* animals are completely defective in 22G biogenesis [37], and we found no evidence for transgenerational antiviral immunity in *rde-3* animals. The ability of *C. elegans* to use a heritable antiviral response to protect offspring from infection represents a fascinating adaptation that warrants further investigation.

The susceptibility of *C. elegans* to VSV provides a genetically-tractable *in vivo* model system to explore negative-sense ssRNA virus biology and antiviral immunity. Our system will nicely complement *in vivo* models that have been established for VSV in *Drosophila* and mice [19], giving investigators the rare opportunity to study a single virus in disparate hosts.

EXPERIMENTAL PROCEDURES

Cell, virus, and worm culture

BHK and BSC-40 cells (from American Type Culture Collection) were cultured as described [24] in Dulbecco's Modified Eagles Medium (DMEM; Invitrogen). VSV stocks were prepared as described [24] and resuspended in DMEM. Viral and nematode strains used in the study are described in Supplemental Experimental Procedures. Unless otherwise indicated, NGM plates were incubated at 25°C for the duration of experiments.

Microinjections

Microinjections used young adults and pulled capillary needles secured onto a Nikon TE-200 microscope equipped with a micromanipulator and regulated pressure source. Needles containing either DMEM (mock-infections) or virus resuspended in DMEM were used for microinjections. Doses of VSV (in PFU) represent estimates based on VSV titration on BSC-40 cells and a dispensed volume of 10 nL during microinjections. Injected worms were immediately placed on NGM plates seeded with OP50 *Escherischia coli*. Where indicated, NGM also contained 50 μg/mL FUdR (Sigma).

RNA isolation and RT-PCR

Total RNA was purified from adult worms or embryos at the indicated times as described [44]. VSV (+)-sense transcription and *C. elegans* actin gene transcription were analyzed by RT-PCR as described [24].

Immunoblotting

Antibodies used for immunoblotting included: mouse anti-LUC (Invitrogen), rabbit anti-actin (Abcam), and mouse anti-VSV Matrix (Dr. Douglas Lyles (Wake Forest School of Medicine, Winston–Salem, NC). Immunoblots were performed as described [24].

Lifespan, LUC, and Transgenerational Immunity Assays, Microscopy, and Small RNA Cloning and Analysis

See Supplemental Experimental Procedures.

Supplementary Material

Refer to Web version on PubMed Central for supplementary material.

Acknowledgments

We thank Dr. Rita Sharma and Ms. Tauny Tambolleo for excellent technical assistance. D.B.G. was supported by fellowships from the Natural Sciences and Engineering Research Council of Canada and Alberta Innovates Health Solutions. C.C.M. was funded by the National Institutes of Health (Grant 5R37GM058800) and is a Howard Hughes Medical Institute Investigator. N.S. was funded by the National Institutes of Health (Grant AI060025). The authors declare that no competing interests exist.

References

1. Zhang R, Hou A. Host-Microbe Interactions in Caenorhabditis elegans. ISRN Microbiol. 2013; 2013:356451. [PubMed: 23984180]

2. Cohen LB, Troemel ER. Microbial pathogenesis and host defense in the nematode C. elegans. Curr Opin Microbiol. 2015; 23:94–101. [PubMed: 25461579]

3. Schott DH, Cureton DK, Whelan SP, Hunter CP. An antiviral role for the RNA interference machinery in Caenorhabditis elegans. Proc Natl Acad Sci U S A. 2005; 102:18420–18424. [PubMed: 16339901]

4. Wilkins C, Dishongh R, Moore SC, Whitt MA, Chow M, Machaca K. RNA interference is an antiviral defence mechanism in Caenorhabditis elegans. Nature. 2005; 436:1044–1047. [PubMed: 16107852]

5. Gammon DB, Mello CC. RNA interference-mediated antiviral defense in insects. Curr Opin Insect Sci. 2015; 8:111–120. [PubMed: 26034705]

6. Szittya G, Burgyan J. RNA interference-mediated intrinsic antiviral immunity in plants. Curr Top Microbiol Immunol. 2013; 371:153–181. [PubMed: 23686235]

7. Maillard PV, Ciaudo C, Marchais A, Li Y, Jay F, Ding SW, Voinnet O. Antiviral RNA interference in mammalian cells. Science. 2013; 342:235–238. [PubMed: 24115438]

8. Li Y, Lu J, Han Y, Fan X, Ding SW. RNA interference functions as an antiviral immunity mechanism in mammals. Science. 2013; 342:231–234. [PubMed: 24115437]

9. Ashe A, Belicard T, Le Pen J, Sarkies P, Frezal L, Lehrbach NJ, Felix MA, Miska EA. A deletion polymorphism in the Caenorhabditis elegans RIG-I homolog disables viral RNA dicing and antiviral immunity. Elife. 2013; 2:e00994. [PubMed: 24137537]

10. Pak J, Fire A. Distinct populations of primary and secondary effectors during RNAi in C. elegans. Science. 2007; 315:241–244. [PubMed: 17124291]

11. Sijen T, Steiner FA, Thijssen KL, Plasterk RH. Secondary siRNAs result from unprimed RNA synthesis and form a distinct class. Science. 2007; 315:244–247. [PubMed: 17158288]

12. Lu R, Maduro M, Li F, Li HW, Broitman-Maduro G, Li WX, Ding SW. Animal virus replication and RNAi-mediated antiviral silencing in Caenorhabditis elegans. Nature. 2005; 436:1040–1043. [PubMed: 16107851]

13. Lu R, Yigit E, Li WX, Ding SW. An RIG-I-Like RNA helicase mediates antiviral RNAi downstream of viral siRNA biogenesis in Caenorhabditis elegans. PLoS Pathog. 2009; 5:e1000286. [PubMed: 19197349]

14. Felix MA, Ashe A, Piffaretti J, Wu G, Nuez I, Belicard T, Jiang Y, Zhao G, Franz CJ, Goldstein LD, et al. Natural and experimental infection of Caenorhabditis nematodes by novel viruses related to nodaviruses. PLoS Biol. 2011; 9:e1000586. [PubMed: 21283608]

15. Franz CJ, Renshaw H, Frezal L, Jiang Y, Felix MA, Wang D. Orsay, Santeuil and Le Blanc viruses primarily infect intestinal cells in Caenorhabditis nematodes. Virology. 2014; 448:255–264. [PubMed: 24314656]

16. Whelan SP, Ball LA, Barr JN, Wertz GT. Efficient recovery of infectious vesicular stomatitis virus entirely from cDNA clones. Proc Natl Acad Sci U S A. 1995; 92:8388–8392. [PubMed: 7667300]

17. Lawson ND, Stillman EA, Whitt MA, Rose JK. Recombinant vesicular stomatitis viruses from DNA. Proc Natl Acad Sci U S A. 1995; 92:4477–4481. [PubMed: 7753828]

18. Liang G, Gao X, Gould EA. Factors responsible for the emergence of arboviruses; strategies, challenges and limitations for their control. Emerg Microbes Infect. 2015; 4:e18. [PubMed: 26038768]

19. Hastie E, Cataldi M, Marriott I, Grdzelishvili VZ. Understanding and altering cell tropism of vesicular stomatitis virus. Virus Res. 2013; 176:16–32. [PubMed: 23796410]

20. Duntsch CD, Zhou Q, Jayakar HR, Weimar JD, Robertson JH, Pfeffer LM, Wang L, Xiang Z, Whitt MA. Recombinant vesicular stomatitis virus vectors as oncolytic agents in the treatment of high-grade gliomas in an organotypic brain tissue slice-glioma coculture model. J Neurosurg. 2004; 100:1049–1059. [PubMed: 15200120]

21. Kern A, Ackermann B, Clement AM, Duerk H, Behl C. HSF1-controlled and age-associated chaperone capacity in neurons and muscle cells of C. elegans. PLoS One. 2010; 5:e8568. [PubMed: 20052290]

22. Guo X, Zhang R, Wang J, Ding SW, Lu R. Homologous RIG-I-like helicase proteins direct RNAi-mediated antiviral immunity in C. elegans by distinct mechanisms. Proc Natl Acad Sci U S A. 2013; 110:16085–16090. [PubMed: 24043766]

23. Roers A, Hiller B, Hornung V. Recognition of Endogenous Nucleic Acids by the Innate Immune System. Immunity. 2016; 44:739–754. [PubMed: 27096317]
24. Gammon DB, Duraffour S, Rozelle DK, Hehnly H, Sharma R, Sparks ME, West CC, Chen Y, Moresco JJ, Andrei G, et al. A single vertebrate DNA virus protein disarms invertebrate immunity to RNA virus infection. Elife. 2014; 3
25. Cureton DK, Massol RH, Saffarian S, Kirchhausen TL, Whelan SP. Vesicular stomatitis virus enters cells through vesicles incompletely coated with clathrin that depend upon actin for internalization. PLoS Pathog. 2009; 5:e1000394. [PubMed: 19390604]
26. Tabara H, Sarkissian M, Kelly WG, Fleenor J, Grishok A, Timmons L, Fire A, Mello CC. The rde-1 gene, RNA interference, and transposon silencing in C. elegans. Cell. 1999; 99:123–132. [PubMed: 10535731]
27. Kim JK, Gabel HW, Kamath RS, Tewari M, Pasquinelli A, Rual JF, Kennedy S, Dybbs M, Bertin N, Kaplan JM, et al. Functional genomic analysis of RNA interference in C. elegans. Science. 2005; 308:1164–1167. [PubMed: 15790806]
28. Winston WM, Molodowitch C, Hunter CP. Systemic RNAi in C. elegans requires the putative transmembrane protein SID-1. Science. 2002; 295:2456–2459. [PubMed: 11834782]
29. Grishok A, Pasquinelli AE, Conte D, Li N, Parrish S, Ha I, Baillie DL, Fire A, Ruvkun G, Mello CC. Genes and mechanisms related to RNA interference regulate expression of the small temporal RNAs that control C. elegans developmental timing. Cell. 2001; 106:23–34. [PubMed: 11461699]
30. Batista PJ, Ruby JG, Claycomb JM, Chiang R, Fahlgren N, Kasschau KD, Chaves DA, Gu W, Vasale JJ, Duan S, et al. PRG-1 and 21U-RNAs interact to form the piRNA complex required for fertility in C. elegans. Mol Cell. 2008; 31:67–78. [PubMed: 18571452]
31. Mitchell DH, Stiles JW, Santelli J, Sanadi DR. Synchronous growth and aging of Caenorhabditis elegans in the presence of fluorodeoxyuridine. J Gerontol. 1979; 34:28–36. [PubMed: 153363]
32. Levine S, Olson W. Nucleic acids of measles and vesicular stomatitis viruses. Proc Soc Exp Biol Med. 1963; 113:630–631. [PubMed: 13930170]
33. Ashe A, Sarkies P, Le Pen J, Tanguy M, Miska EA. Antiviral RNA Interference against Orsay Virus Is neither Systemic nor Transgenerational in Caenorhabditis elegans. J Virol. 2015; 89:12035–12046. [PubMed: 26401037]
34. Rechavi O, Minevich G, Hobert O. Transgenerational inheritance of an acquired small RNA-based antiviral response in C. elegans. Cell. 2011; 147:1248–1256. [PubMed: 22119442]
35. Sterken MG, Snoek LB, Bosman KJ, Daamen J, Riksen JA, Bakker J, Pijlman GP, Kammenga JE. A heritable antiviral RNAi response limits Orsay virus infection in Caenorhabditis elegans N2. PLoS One. 2014; 9:e89760. [PubMed: 24587016]
36. Chen CC, Simard MJ, Tabara H, Brownell DR, McCollough JA, Mello CC. A member of the polymerase beta nucleotidyltransferase superfamily is required for RNA interference in C. elegans. Curr Biol. 2005; 15:378–383. [PubMed: 15723801]
37. Shirayama M, Seth M, Lee HC, Gu W, Ishidate T, Conte D Jr, Mello CC. piRNAs initiate an epigenetic memory of nonself RNA in the C. elegans germline. Cell. 2012; 150:65–77. [PubMed: 22738726]
38. Kato H, Takeuchi O, Sato S, Yoneyama M, Yamamoto M, Matsui K, Uematsu S, Jung A, Kawai T, Ishii KJ, et al. Differential roles of MDA5 and RIG-I helicases in the recognition of RNA viruses. Nature. 2006; 441:101–105. [PubMed: 16625202]
39. Sabin LR, Zheng Q, Thekkat P, Yang J, Hannon GJ, Gregory BD, Tudor M, Cherry S. Dicer-2 processes diverse viral RNA species. PLoS One. 2013; 8:e55458. [PubMed: 23424633]
40. Anderson EN, Corkins ME, Li JC, Singh K, Parsons S, Tucey TM, Sorkac A, Huang H, Dimitriadi M, Sinclair DA, et al. C. elegans lifespan extension by osmotic stress requires FUdR, base excision repair, FOXO, and sirtuins. Mech Ageing Dev. 2016; 154:30–42. [PubMed: 26854551]
41. Troemel ER, Felix MA, Whiteman NK, Barriere A, Ausubel FM. Microsporidia are natural intracellular parasites of the nematode Caenorhabditis elegans. PLoS Biol. 2008; 6:2736–2752. [PubMed: 19071962]
42. Jobson MA, Jordan JM, Sandrof MA, Hibshman JD, Lennox AL, Baugh LR. Transgenerational Effects of Early Life Starvation on Growth, Reproduction, and Stress Resistance in Caenorhabditis elegans. Genetics. 2015; 201:201–212. [PubMed: 26187123]

43. Rechavi O, Houri-Ze'evi L, Anava S, Goh WS, Kerk SY, Hannon GJ, Hobert O. Starvation-induced transgenerational inheritance of small RNAs in C. elegans. Cell. 2014; 158:277–287. [PubMed: 25018105]

44. Gu W, Shirayama M, Conte D Jr, Vasale J, Batista PJ, Claycomb JM, Moresco JJ, Youngman EM, Keys J, Stoltz MJ, et al. Distinct argonaute-mediated 22G-RNA pathways direct genome surveillance in the C. elegans germline. Mol Cell. 2009; 36:231–244. [PubMed: 19800275]

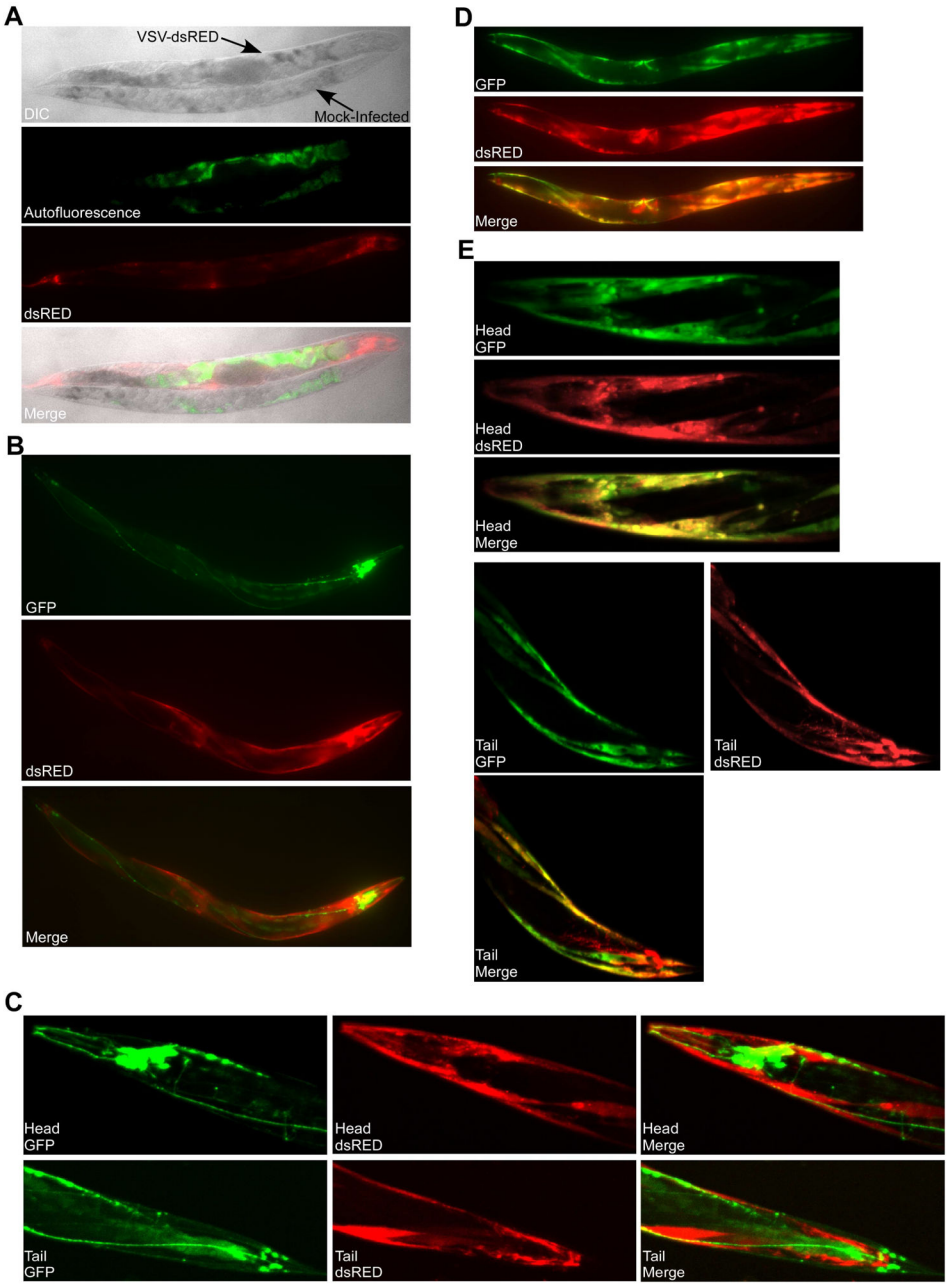

Figure 1. Microinjection of adult *C. elegans* animals with recombinant vesicular stomatitis virus (VSV) expressing dsRED (VSV-dsRED) results in an infection primarily restricted to muscle tissue

(A) Differential interference contrast (DIC) and fluorescence micrographs (10X magnification) of N2 adults either mock- or VSV-dsRED-infected. Images were taken 72 hours post-infection (hpi). Green fluorescence indicates autofluorescence signal in the intestine. (B) Fluorescence micrographs (10X magnification) of *psng-1*::LUC-GFP adult infected with VSV-dsRED 72 hpi. (C) Confocal microscopy fluorescence micrographs (20X magnification) of head and tail regions of a p*sng-1*::GFP-LUC adult infected with VSV-dsRED 72 hpi. (D) Fluorescence micrographs (10X magnification) of p*myo-3*::LUC-GFP

adult infected with VSV-dsRED 72 hpi. (E) Confocal microscopy fluorescence micrographs (20X magnification) of head and tail regions of a p*myo-3*::GFP-LUC adult infected with VSV-dsRED 72 hpi. All infections were carried out using 10^4 plaque forming units (PFU) of VSV-dsRED per injection. See also Figure S1.

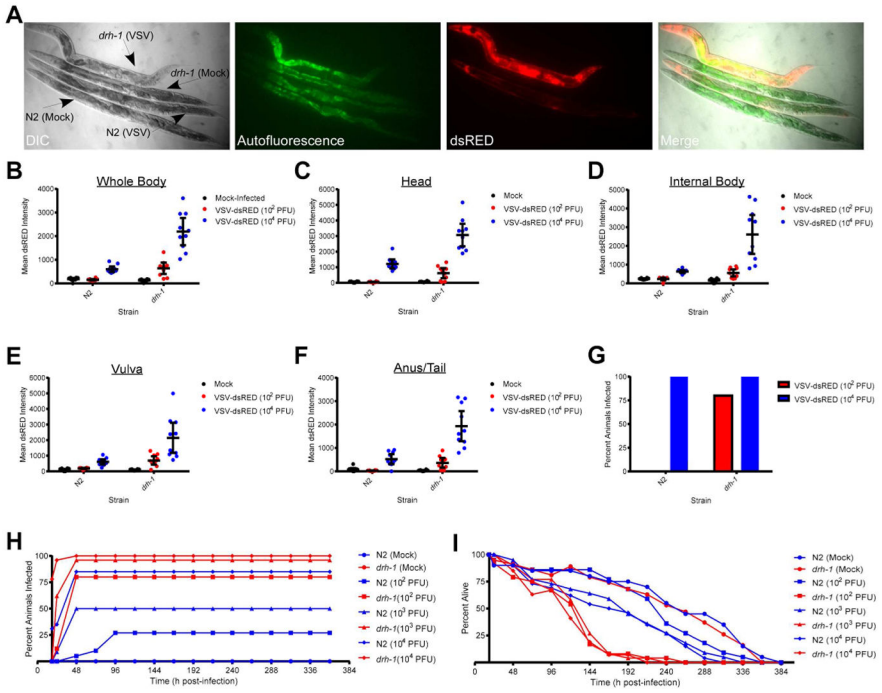

Figure 2. Loss of Dicer-related helicase 1 (DRH-1) function results in enhanced susceptibility to VSV-dsRED infection

(A) Differential interference contrast (DIC) and fluorescence micrographs (10X magnification) of N2 or *drh-1* adults mock-infected or infected with 10^4 PFU of VSV-dsRED. Images were taken 72 hpi. Green fluorescence indicates autofluorescence obtained in the intestine. (B–F) Mean dsRED intensity measurements for N2 or *drh-1* adults (n = 10/treatment) 48 hpi using the indicated VSV-dsRED dose. Measurements were taken of either the whole body (B) or of the indicated tissues (C–F). Mean dsRED measurements for the entire group (horizontal bar) and 95% confidence intervals (error bars) are shown. (G) Percentage of animals displaying a whole body dsRED signal at least two-fold above mock-infected animals by 48 hpi. (H) Percentage of animals (n = 20–30/treatment) displaying dsRED signal at the indicated times post-infection. (I) Percentage of animals from (H) alive at the indicated times post-infection. See also Figures S2–3.

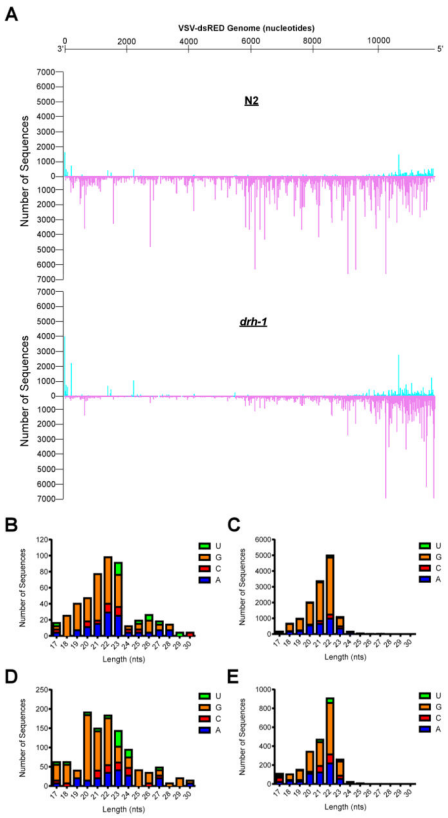

Figure 3. Small RNAs produced upon VSV-dsRED Infection of N2 and *drh-1* animals

(A) The number of unique sequences obtained by Illumina high-throughput small RNA sequencing that match a given position in the VSV-dsRED genome in infected N2 or *drh-1* animals is shown. The number of unique sequences in sense and antisense orientation are shown on the positive (cyan) and negative (purple) *y*-axis, respectively. The negative-sense ssRNA VSV-dsRED genome (in 3′-to-5′ orientation) is depicted above. (B–C) Features of sense (B) and antisense (C) small RNAs (length and identity of first nucleotide) cloned from VSV-dsRED-infected N2 animals. (D–E) Features of sense (D) and antisense (E) small RNAs cloned from VSV-dsRED-infected *drh-1* animals.

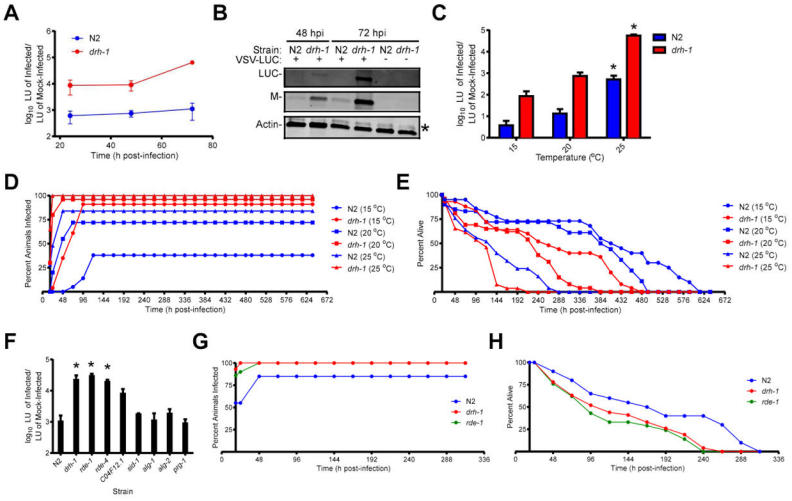

Figure 4. Characterization of the effect(s) of nematode culturing temperature and host genetic background on VSV replication and host survival

(A) Luciferase (LUC) assay [in arbitrary light units (LU)] of adult animals (n =15/treatment/experiment) infected with 10^4 PFU of VSV-LUC. LU detected from infected animals were divided by LU obtained from mock-infected animals of the same strain. Data represent means (± SEM). (B) Immunoblot of lysates from (A) for LUC, VSV Matrix (M), and cellular actin proteins. The asterisk indicates a non-specific band in the actin immunoblot. (C) LUC assay of lysates from adult animals (n = 10/treatment/experiment) infected with 10^4 PFU of VSV-LUC and cultured at the indicated temperatures until 72 hpi. Data represent means (+ SEM) and asterisks indicate treatments that are significantly different ($P<0.05$) from 15°C treatments within strains. (D) Percentage of animals (n = 20–30/treatment) displaying dsRED signal at the indicated times post-infection with 10^4 PFU VSV-dsRED. (E) Percentage of animals from (D) alive at the indicated times post-infection. (F) LUC assay of lysates from adult animals (n =10/treatment/experiment) infected with 10^4 PFU of VSV-LUC until 72 hpi. LU detected from infected animals were divided by LU obtained from mock-infected N2 animals. Data represent means (+ SEM) and asterisks indicate treatments that are significantly different ($P<0.05$) than N2 treatments. (G) Percentage of animals (n = 20–30/treatment) displaying dsRED signal at the indicated times post-infection with 10^4 PFU VSV-dsRED. (H) Percentage of animals from (G) alive at the indicated times post-infection.

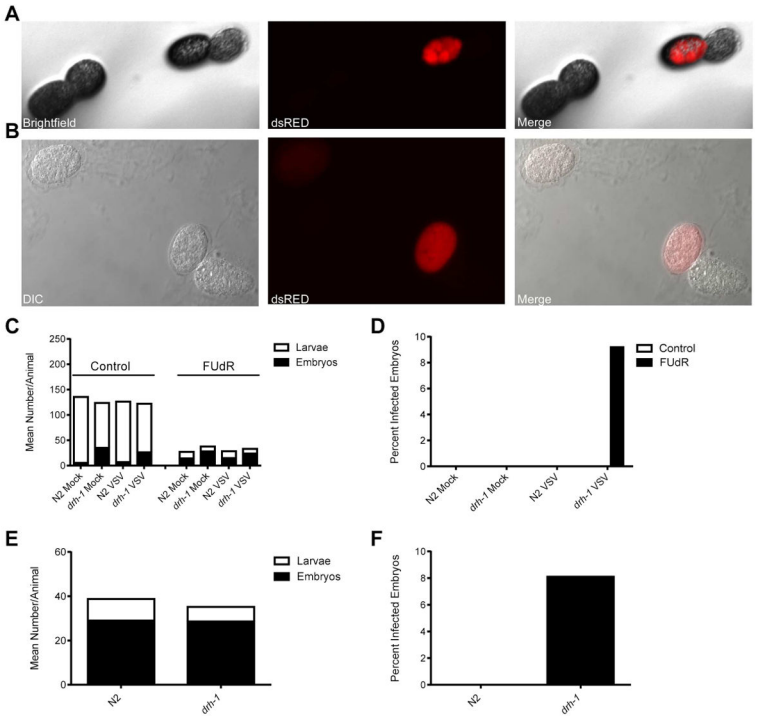

Figure 5. DRH-1 is required for full immunity to vertical virus transmission

(A) Brightfield and fluorescence micrographs (112X magnification) taken with a fluorescence stereo zoom microscope of a dsRED-positive embryo laid by an adult *drh-1* animal infected with VSV-dsRED. (B) Differential interference contrast and fluorescence micrographs (40X magnification) of dsRED-positive embryos laid by an adult *drh-1* animal infected with VSV-dsRED. (C) Mean number (+SEM) of larvae or dead embryos laid by mock- or VSV-dsRED-infected animals (n = 10 animals/treatment) 48 hpi when cultured on normal nematode growth media (control) or media containing Fluorodeoxyuridine (FUdR). (D) Percentage of total embryos from (C) displaying dsRED signal. (E) Mean number of larvae or dead embryos laid by VSV-dsRED-infected animals (n = 20 animals/treatment) 48 hpi when cultured on plates containing FUdR. (F) Percentage of total embryos from (E) displaying dsRED signal. See also Figures S4–6.

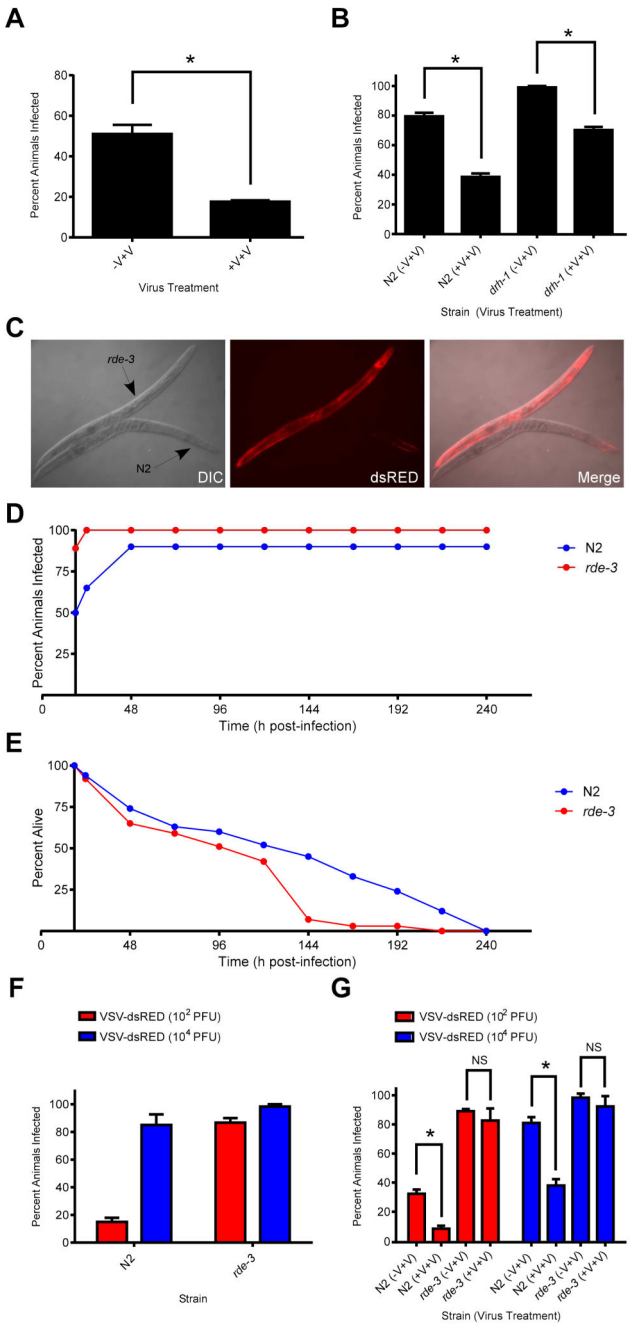

Figure 6. Prior exposure of parental animals to virus infection confers protective immunity to their progeny that is dependent on RDE-3

(A) Percentage of progeny animals collected from mock- (−V+V) or VSV-dsRED-infected (+V+V) mothers displaying dsRED signal 96 hpi with 10^3 PFU of VSV-dsRED. (B) Percentage of N2 or *drh-1* progeny animals collected from mock- (−V+V) or VSV-dsRED-infected (+V+V) mothers displaying dsRED signal 72 hpi with 10^4 PFU of VSV-dsRED. (C) Differential interference contrast (DIC) and fluorescence micrographs (10X magnification) of N2 or *rde-3* adults infected with 10^4 PFU of VSV-dsRED. Images were taken 72 hpi. (D) Percentage of animals displaying dsRED signal at the indicated times post-

infection with 10^4 PFU VSV-dsRED. (E) Percentage of animals from (D) alive at the indicated times post-infection. (F). Percentage of N2 or *rde-3* animals displaying dsRED signal at 72 hpi after challenge with the indicated doses of VSV-dsRED. (G) Percentage of N2 or *rde-3* progeny animals collected from mock- (−V+V) or VSV-dsRED-infected (+V +V) mothers displaying dsRED signal 72 hpi after challenge with either 10^2 or 10^4 PFU of VSV-dsRED. All quantitative experiments used 20–30 animals/treatment and data in bar graphs represent means (+ SEM). Where statistical analyses were performed, asterisks indicate treatments that are significantly different ($P<0.05$) from control (−V+V) treatments.